Power control optimization of a new contactless piezoelectric harvester

Ekaitz Zulueta [a,], Erol Kurt [b], Yunus Uzun [c], Jose Manuel Lopez-Guede [a]*

[a] Department of Systems Engineering and Control, University College of Engineering at Vitoria-Gasteiz, University of the Basque Country UPV/EHU, Vitoria-Gasteiz, Spain
[b] Department of Electrical and Electronics Engineering, Technology Faculty, Gazi University, TR-06500, Beşevler, Ankara, Turkey
[c] Department of Electrical and Electronics Engineering, Faculty of Engineering, Aksaray University, Aksaray, Turkey

ARTICLE INFO

ABSTRACT

In this study, we propose an optimization scheme for the control of a piezoelectric wind energy harvester. The harvester is constructed by a blade in front and a magnet in the rear in order to sustain a magnetic repulsion by another magnet located on the stable harvester body in a contactless manner. For such a new harvester, the control scheme is missing in the literature in the sense that the harvester is new and an overall optimization study is required for such a device. In that context, the optimization has been realized by using a new current control law based on the harvester piezoelectric terminal voltage and the layer bending. The proposed control law can impose a second order linear dynamics although the magnetic effects can yield to nonlinear magnetic force relation. In order to improve the new control strategy, a Particle Swarm Optimization algorithm (PSO) has been applied, since there is a nonlinear dependency among the control parameters, the collected energy and the bending force mean values. According to results, the captured electrical power has a high increasing trend with respect to the only-voltage-based (OVB) control as the current study proves. On the contrary, the artifact of the method is that the obtained power is too low to increase the mean bending forces and it requires much complicated control system.

Introduction

In order to supply the increased demand of energy caused by the population growth and greater power consumption, invention of new energy harvester systems and their optimization have become key points for a few decades. Indeed, when the issue is to construct optimized energy harvester systems, the balance between demand and supply is also vital problem to deal from a multidisciplinary view. It is desirable to obtain sustainable, safe and world-wide applicable methods [1–3]. Before 2000's, the most of energy supply was based on fossil fuels working in so-called conventional energy systems. However, both the limitations in the supply and the globally inhomogeneous distribution make the usage of those fuels inefficient.

The combination of solar and wind energy systems has become an alternative research and practice area [4]. Similarly, a study made by Ref. [5] proposed an energy generation model that includes factors such as emissions reduction, minimization of imported energy and social acceptance.

In the frame of low power systems, a significant increase has been experimented; indeed energy harvesting systems in that power scale allows energy supplies for low power electronic equipment such as wireless sensors, pacemakers and health monitoring systems. In the last decades, these low power systems have been invented or improved to be operated even without any battery. In addition, harvesters have served as an auxiliary power device, which enhances the life time of the batteries with suitable maximal power point tracking mechanisms [6—9].

In principle, all harvester systems are designed to obtain electrical power from ambient and they transform it into a utilizable form of energy for low power devices. Several energy harvesting methods such as vibration, solar, thermal gradient, etc. have been developed during the last years [6,10,11]. There are many ambient vibrations such as human and machine motions, wind or seismic actions in the environment.

Energy harvesting could be a feasible alternative for micro powering with the main advantage of no need to replace batteries. Power sources could be find in photons (light, infrared, radio frequencies), kinetics schemes (vibrations, human motion, wind power, hydropower) and thermal systems using the temperature gradients [12]. The most important benefits of energy harvesting are based on long lasting operability, cost effective, usually free of maintenance and no need of charging points. Additionally, these systems are very useful in applications for hard natural conditions.

Vibrations can be converted into energy by several techniques: electromagnetic, electrostatic/capacitive and piezoelectric [13]. Among the aforementioned techniques, piezoelectric have some advantages: high power density and voltage. Furthermore, the piezoelectrics are suitable to be optimized for a certain excitation frequencies and that can help to increase the system efficiency drastically [14,15]. The materials used for piezoelectric conversion are naturally-occurring ones as crystals (Quartz, Rochelle salt), ceramics and polymers [16—18].

The main objective of the paper is to show how a novel optimization system has been used in order to increase the captured energy by energy harvesting. Due to this objective, a new piezoelectric control law has been designed using swarm optimization algorithms. In the literature, there are a number of control algorithms which try to increase the captured power like [19]. In our study, we have introduced the voltage and the deflection of piezoelectric beam which highly enhances the mean power captured by the energy harvester.

The paper is structured as follows: the second section presents the main objectives and the general schema of the wind energy harvester. In the third section the energy harvester model has been explained and the proposed control law in this analyzed. The fourth section is devoted to design the optimization algorithm, describing the general steps and the cost function, while the obtained results are discussed in the fifth section. Finally, the last section gives our main conclusions.

The wind energy harvester

The energy harvester used in this work has been developed by the Alternative Energy Researches Group of Gazi University and some preliminary findings and features of the device have
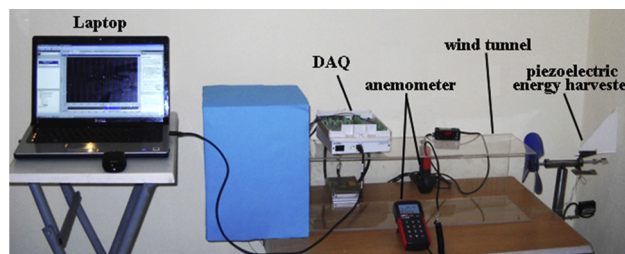

Fig. 1 — The harvester and the wind tunnel test setup.

been reported in previous papers [20,21]. This system shown in Fig. 1 has a wind turbine that collects the energy from the wind and induces a bending deflection by the help of two permanent magnets (one in the rotor side and other in the piezoelectric beam).

The tests of the system can be easily realized by using a small wind tunnel, an anemometer, the harvester, a data acquisition card (DAQ) and a laptop. The system enables us to record the data (i.e., harvested voltage, deflection, velocity and acceleration) with high precision.

This set of permanent magnets let us to build a contactless energy transfer between the wind turbine axis and the piezoelectric system, eliminating the physical damages due to any contact with a shaft. In this work, the control law has been proposed in order to improve the bending and the collected power. The control law has mainly two inputs: the piezoelectric terminal voltage and the bending deflection.

In comparison with previous works [21], the control law can completely impose the second order dynamics. Therefore, the control law parameters have been optimized by a Particle Swarm Optimization (PSO) algorithm, because there is a nonlinear dependency between the control law parameters and the cost function. The cost function takes into account the mean power harvested and the mean bending force obtained in different wind turbine regimes.

Problem statement

The main problem to solve in this paper is to increase the mean power captured by changing the control law and to optimize the control parameters by using a Particle Swarm Optimization algorithm (PSO). Within that frame, initially the block diagram of the present work is presented in Fig. 2.

Here, the inputs and outputs are defined in Tables 1 and 2. The main problem is to choose an appropriate cost function, since it should be strongly linked to the objective that is pursued. In this case, the objective is to increase the power captured by the harvester as the first step. In addition to that energy increasing objective, we should keep the bending force less enough. That is also important to prevent the piezoelectric layer from any damage.

In the optimization cost function, we have proposed a proportionally inverse value to the mean captured power. The mean bending force have been applied as the inequality restriction. If a certain upper bound is found, the cost function is highly increased; otherwise the cost function is proportionally decreased by considering the mean captured power. The
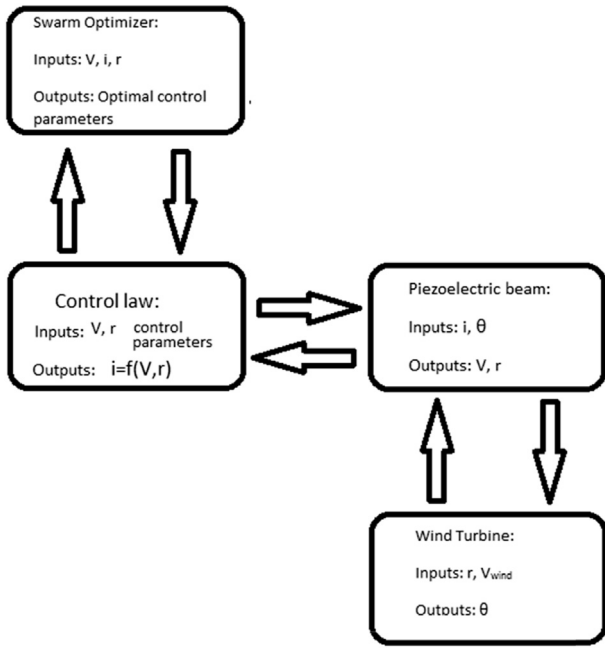
Fig. 2 — System block diagram.

Table 1 — Model parameters.

Name	Definition	Value	Units
ρ	Material density	5319	$kg\ m^{-3}$
ρ_{air}	Air density	1.225	$kg\ m^{-3}$
A	Section of piezoelectric	0.0001645	m^2
k	Piezoelectric stiffness	123	$N\ m^{-1}$
K_{trans}	Transduction gain	0.006	$rad\ m^{-1}$
	Piezoelectric force factor		
F_m	Magnetic force strength	0.2460	N
C	Piezoelectric capacitance	232	nF
θ_p	Angular position of magnet	0	rad
$C_p(\lambda)$	Wind turbine power coefficient	See Fig. 4	—
f	Frictional coefficient	10	$Nms\ rad^{-1}$
R_{wt}	Wind turbine radius	0.0850	M
R_{wtdisc}	Piezoelectric radial position	0.01	M
α	Voltage induced bending factor	0.0001	$N\ rad^{-1}$
J_{wt}	Rotor inertia	0.1	$g\ m^3$

proposed cost function has no direct analytic expression because of two main reasons: First, the nonlinearity due to magnetic forces in Eqs. (1)—(6). Second, the wind speed has high stochastic behavior. In the present case, we have used a wind speed simulator called Turbsim [22], with a Normal Turbulence Model in order to form the wind regime.

Wind energy harvester modeling

The harvester model used in this work is based on the modeling proposed in Ref. [21]. The main variables are the wind speed (V_{wind}), the wind turbine rotor speed (ω), the electrical current (i) and the voltage for the piezoelectric element (V). The first two variables are the most important inputs of the system, while the rest are the most important

Table 2 — Model variables.

Name	Definition	Units
r	Propeller deflection angle	rad
V	Piezoelectric voltage	Volts
θ	Wind turbine rotor angle	rad
V_{wind}	Wind speed	$m\ s^{-1}$
ω	Rotor speed	$rad\ s^{-1}$
T_m	permanent magnet torque	Nm
T_{aero}	Aerodynamic torque t	Nm
λ	Tip Speed Ratio (TSR)	—
i	Piezoelectric current	*Amp*

outputs. The harvester model is described by equations from Eqs. (1)—(7):

$$L\rho A \frac{d^2 r}{dt^2} = -k\frac{r}{K_{trans}} - \alpha V + F_m \delta(\theta - \theta_p) \tag{1}$$

$$i = \frac{\alpha}{K_{trans}}\frac{dr}{dt} - C\frac{dV}{dt} \tag{2}$$

$$J_{wt}\frac{d\omega}{dt} = T_{aero} - T_m - f\omega \tag{3}$$

$$T_{aero} = \frac{1}{2}\pi\rho_{air}R_{wt}^2\frac{V_{wind}^3}{\omega}C_p(\lambda) \tag{4}$$

$$\lambda = \frac{\omega\ R_{wt}}{V_{wind}} \tag{5}$$

$$T_m = F_m\delta(\theta - \theta_p)\ R_{wtdisc}\ sin(\theta - \theta_p) \tag{6}$$

$$\frac{d\theta}{dt} = \omega \tag{7}$$

$$\delta(\theta - \theta_p) = \begin{cases} 1 & : \quad when\ \ \theta = \theta_p \\ 0 & : \quad else \end{cases} \tag{8}$$

Here, the model parameters and system variables are defined in Tables 1 and 2, respectively. The Eq. (8) is a Kronecker like function and it is 1, when $\theta = \theta_p$ otherwise it is 0. The deflection is given by the radial distance from the equilibrium and denoted by r. The layer piezoelectric length is given by L and can be changed by the manufacturer. The magnetic force exerted by the repulsion of the magnets is represented by F_m. This model can present a complicated time-dependent behavior due to the stochastic nature of the wind. According to literature, some piezoelectric-based energy harvesters indicate a rich chaotic behavior, and that is more intrinsic than in the present case, since the system has a hard sensibility to some mechanics parts like in Ref. [23]. For instance, in Ref. [24], there is a remarkable study about the wind turbine tower dynamics and its control in order to reduce the fore-after tower dynamics induced by the electrical generator.

When a complicated system is to be analyzed, a parameter sensibility analysis can be interesting in order to quantify the parameter error effect. In the following works [25—27], there are some parameter sensibility analysis which have been applied to energy harvesters. But in the case of the current study, the system has no chaotic behavior. The chaotic
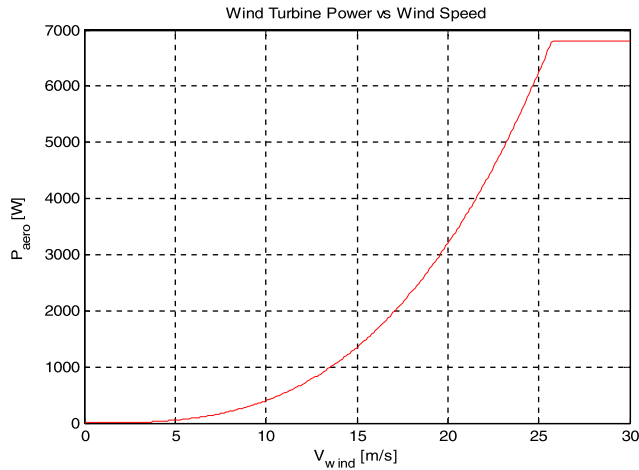
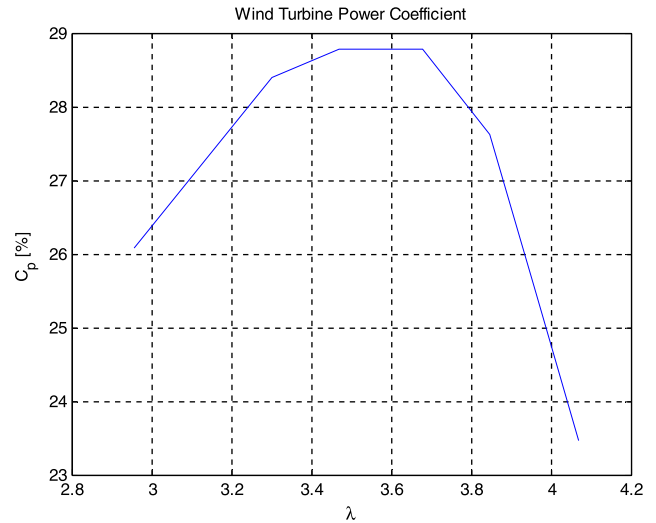Fig. 3 — **Wind turbine mechanical power *vs* wind speed.**

Fig. 4 — **Wind turbine power coefficient *vs* Tip Speed Ratio (λ).**

behavior appears due to the stochastic nature of wind. Hence, this system does not need a parameter sensibility analysis. Eq. (12) shows a second order linear dynamics, which in comparison the Duffing equation, the first one has not a high order or third order term. Indeed, this term induces a chaotic behavior in the literature, which does not exist in our system such as [28,29].

The system variables mainly consist of the mechanical and wind-related terms and form the relation between the propeller and the harvested electrical energy.

The wind turbine used in this paper has been modeled following [30], and its more relevant parameters and variables are shown in Figs. 3 and 4.

According to Fig. 3, the aerodynamic power increases rapidly for a wind speed range and beyond a wind speed of 26 ms^{-1}, it is fixed to P = 6.800 W. According to that model, Fig. 4 shows that the turbine power coefficient increases up from 26% to 28.9% (peak value) and decreases rapidly to 23.5% with respect to the Tip Speed Ratio (λ).

In this work four different wind speed regimes have been used. The wind speed sequences have been simulated by Turbsim, an NREL designed tool [22], using the IECKAI model (Kaimal Turbulence Model), with a C class (12%) and Normal Turbulence Model level. The wind speed realizations have been simulated with the following parameters: time step and span are adjusted to 0.01 s and 400 s respectively. We have carried out different simulations with different wind mean speed values (i.e., $v_w = 5$, 10, 20 and 25 ms^{-1}) in order to assess the suitability of the reached results for a wide range of wind speed values.

This harvester is capable to extract much more power from the wind than the load needs. Usually the rotor friction slows down the rotor speed. The main objective is to gain as much as possible of energy. The counterpart of a high energy capture is the increasing of the bending force applied to piezoelectric beam by the permanent magnet.

Voltage and deflection based current control

In the previous works [14,22], the piezoelectric current adjustment is imposed by a piezoelectric voltage based

proportional control. We introduce a much more general control law, because the control dynamics is not completely imposed trough OVB control as proposed in Ref. [21]. The new control algorithm of the control law is more general and lets us to impose Eq. (9):

$$i = Kp_v V - Kp_r r, \tag{9}$$

where Kp_v and Kp_r are the control parameters that we can tune.

This control law has been proposed since it is simple enough and at the same time the closed loop dynamics can be completely imposed (see Eqs. (10)—(13)). On one hand, the voltage term lets us to change the damping factor, while on the other hand the bending deflection term lets us to impose the natural frequency. Therefore, the control law is summarized in Fig. 5. This control law determines the current depending on the voltage in order to detect when the energy can be acquired from wind turbines axis, and the position term let to the control imposes certain natural frequency value. Due to the fact that the power is depending on voltage and current product, it looks reasonable to propose a current control law that depends on voltage.

Closed loop dynamic analysis

The equivalent closed loop is a second order system. The first approximation can be written as indicated by Eqs. (10) and (11), because the voltage time constant is much faster than the mechanical dynamics.

$$i \approx \frac{\alpha}{K_{trans}} \frac{dr}{dt} \tag{10}$$

$$Kp_v V - Kp_r r = \frac{\alpha}{K_{trans}} \frac{dr}{dt} \tag{11}$$

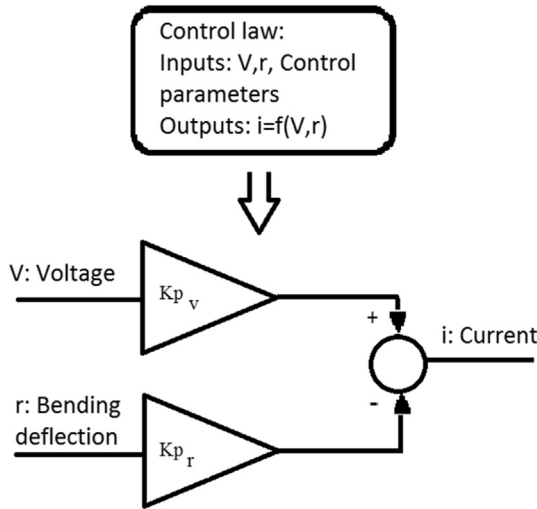Eq. (11) can be combined with Eq. (1), and we can also see in Eq. (12).

Fig. 5 — **Proposed control law.**

$$L_1 \rho A \ddot{r} + \frac{\alpha^2}{Kp_v \cdot K_{trans}} \dot{r} + \left(\frac{k}{K_{trans}} + \frac{\alpha Kp_r}{Kp_v} \right) r = u,$$ (12)

where the input signal u is defined as follows by Eq. (13) in terms of magnetic force:

$$u = F_m \delta (\theta - \theta_p)$$ (13)

Eq. (12) is a second order linear differential equation, whose coefficients can be imposed by a correct set of parameters values. The relationship between the mean power captured by the harvester and the control parameters is obvious. Other important problem is to define the relationship between the bending force and it is addressed in the next section.

Swarm optimization of the energy harvester control

The control law introduced in this paper is based on two parameters: Kp_v and Kp_r, as stated in Eq. (9). These two parameters have become the dynamics between the magnetic force and the piezoelectric beam deflection in a linear form. Besides, the relationship between the mean captured power and these control parameters are not known. So, when one has to choose the control parameters values pursuing the optimal solution, one should try a number of solutions and evaluate the results. However, this procedure can be done a number of times, i.e., only if the parametric space is very small.

In the present case, we have two parameters and a lot of pair values can be possible, so an algorithm is required in order to optimize this problem. These considerations have been widely taken into account in other studies [31–34].

We have applied the PSO algorithm instead of a gradient descendent algorithm, since the cost function has not analytical expression depending directly on the Kp_v and Kp_r control parameters as shown in Fig. 6.
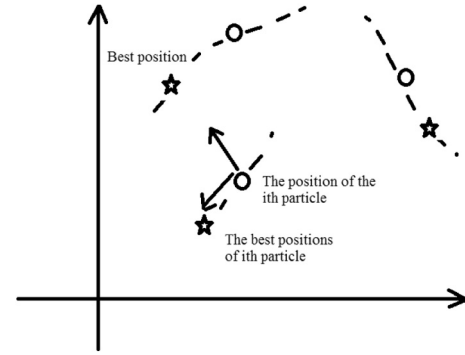

Fig. 6 — **PSO algorithm parameter space.**

There is no analytical expression for the cost function that shows the dependences between the mean captured power and the control parameters. There exist many other intelligent optimization algorithms like differential evolution [35], back search tracking searching algorithm [36] or neural approaches [37], that could fit well to the current problem. We have tried to solve the problem using them, but they took too much time to converge to an optimal value due to the fact that these algorithms search solutions in a much random fashion. In this problem the cost function is a smooth surface as it will be plotted in Fig. 7.

Another important issue is related to the constraints definition. In this problem we have only one constraint, the mean value of bending force that can be hold by the piezoelectric beam. In this case, the constraint is an inequality.

Optimization problem

Any optimization algorithm has several general issues that must be considered:

a) The stop conditions, for example, maximum iterations, the maximum acceptable goal value, the minimum acceptable goal change between two consecutive iterations, etc. In
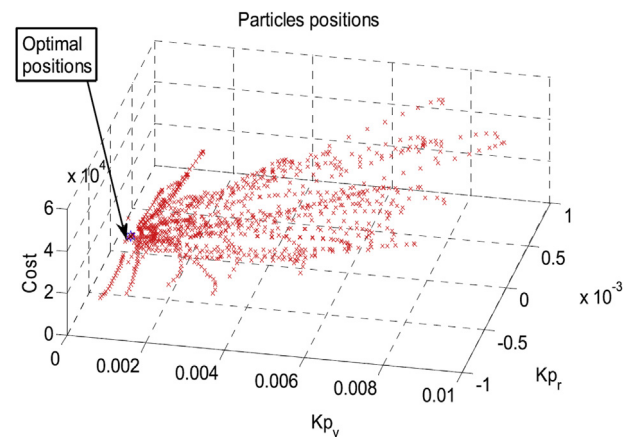

Fig. 7 — **Particle trajectories generated through the proposed cost function.**

Table 3 — PSO optimization algorithm parameters.

Name	Definition	Value	Units
I_i	ith particle inertia	0.9	—
$\varphi_{1,max}$	Maximum value for exploration term	1	—
$\varphi_{2,max}$	Maximum value for exploitation term	2	—
dt	Position actualization term	0.01	—
N iter	Maximum number of iterations	20	—
N particles	Number of particles	50	—

Table 4 — PSO optimization algorithm variables.

Name	Definition	Units
$V_i(t)$	ith particle speed at iteration t	—
$X_i(t)$	ith particle position at iteration t	—
$X_{best}(t)$	The best position at iteration t	—
$X_{i,best}(t)$	ith particle best position	—
φ_1	Uniform random value between 0 and $\varphi_{1,max}$	—
φ_2	Uniform random value between 0 and $\varphi_{2,max}$	—

this optimization problem we have used only a maximum number of iterations.

b) The cost function and its constrains. In this case, as we have commented before, the cost function is the proportionally inverse value of the mean captured value. We have an inequality constrain that fixes the maximum bending force.

c) The optimization procedure of the control parameters following these steps:

1. Initialization step: Generation of the possible solutions set. Each solution has two values (The control parameter set: Kp_v and Kp_r). This value set is the position vector of each solution. Each solution in PSO algorithm is called particle. After particle position generation, each particle is evaluated by simulations in a very high mean wind speed. Because if the possible solution gives a good mean power at a high speed, the system gives good mean power values (obviously the captured values are less when the wind speed is lower). The bending maximum values are evaluated, and if the maximum value is reached the cost is highly increased.

2. We proposed different solutions taking into account the positions and the cost values of each particle. These all new positions are evaluated by a simulation. The new solutions are proposed using from Eqs. (14)—(16).

3. The step number two is repeated until a stop conditions is reached. Here, we have applied a maximum number of iterations only.

Special questions should be explained related to the simulation. The dynamical model has been simulated with a 10 s time span when we have executed the optimization procedure, because PSO is a complex algorithm demanding many simulation executions. Thereby, in order to limit the time to achieve a good optimization, we have limited the time span to 10 s. When we have obtained the optimal values given

Table 5 — PSO optimization algorithm cost function parameters.

Name	Definition	Value	Units
T	Time span	10	s
$F_{b,max}$	Maximum mean bending force	0.038	N

by the optimizer, we have made the simulations with 400 s time span, because it is sufficiently long time to see the stationary response of harvester.

Particle Swarm Optimization introduction

The PSO is a well known algorithm and it has been applied successfully in many control problems and other optimization domains since PSO was proposed in Ref. [38], like [39—44]. However, we have not found that this algorithm has been applied to so low power energy harvester for the sake of the control optimization.

The PSO algorithm optimizes a cost function defining a set of particles. Each particle has a position vector and a cost value associated to this position. The position vector components are the values of the optimized variables.

In our case, the control parameters Kp_v and Kp_r are the position components. The cost function is explained in the following section. Each particle stores the best position that has achieved and the cost achieved. Each iteration all particles actualize their speed and positions in the parametric space with the following equations.

$$V_i(t + 1) = I_i \, V_i(t) + \varphi_1 \, (X_{i,best}(t) - X_i(t)) + \varphi_2 \, (X_{best}(t) - X_i(t))$$
(14)

$$X_i(t + 1) = X_i(t) + dt \, V_i(t)$$
(15)

In Tables 3 and 4, the PSO algorithm parameters and variables are defined. Note that the vector form of the position of a particle can be described by Eq. (16):

$$X_i(t) = [Kp_v \, , Kp_r \,]_i$$
(16)

The sub-index *i* refers to the particle or solution and the evolution of the optimal solution searching algorithm is shown in Fig. 7.

Proposal for cost function and constraints

The cost function is defined as follows by Eq. (17):

$$Cost = \begin{cases} \dfrac{1}{T} \displaystyle\int_0^T V \cdot i \cdot dt & F_b < F_{b,max} \\[2ex] \infty & F_{b,max} \le F_b \end{cases}$$
(17)

where F_b is the mean bending force applied by the permanent magnet and exerted to the piezoelectric beam.

$$F_b = \frac{1}{T} \int_0^T F_m \delta(\theta - \theta_p) \cdot dt$$
(18)

Table 5 gives the PSO optimization algorithm details of the cost function parameters.

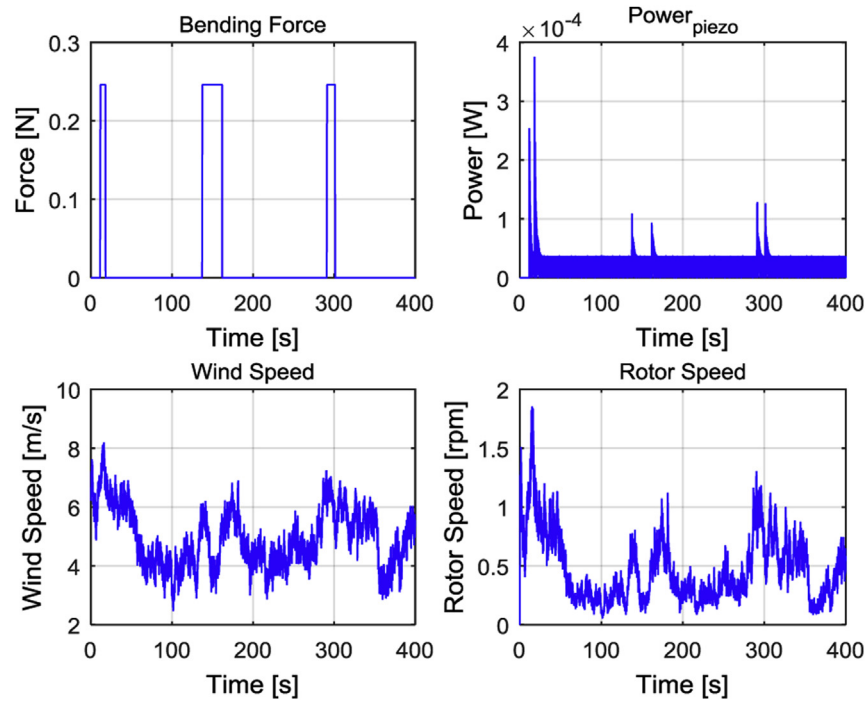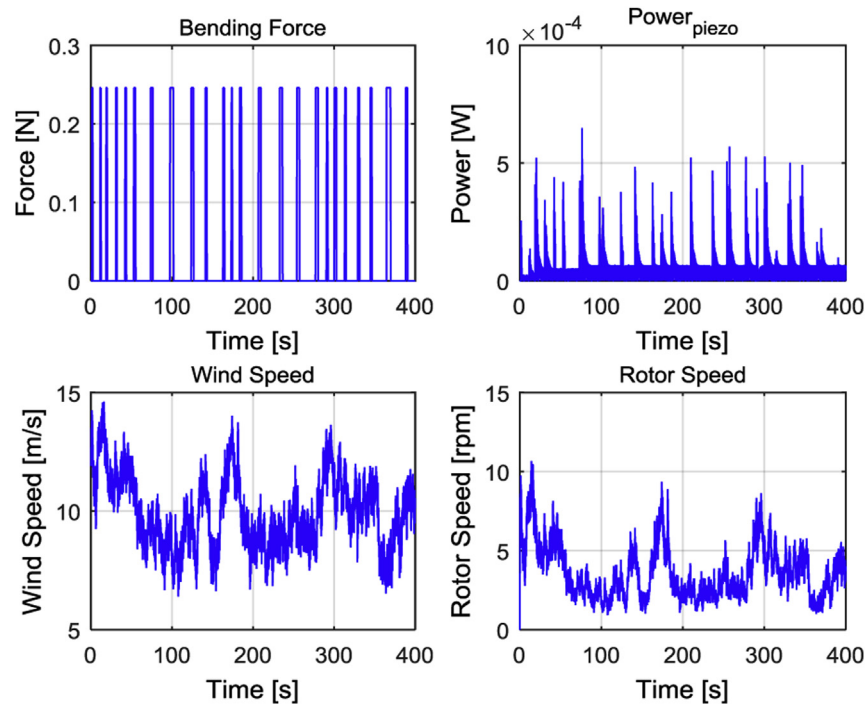**Fig. 8 – Energy harvester response at 5 ms^{-1} wind speed.**

Fig. 9 – Energy harvester response at 10 ms^{-1} wind speed.

Optimization and simulation parameter values

The optimization algorithm has been executed with different parameters such as the number of particles and maximum number of iterations. We have used different values for the mean captured power and the mean bending force to the algorithm. We have limited the simulations to the first 10 s; otherwise they could take too much time. We have chosen only 20 iterations and 50 particles in order to find optimized parameters as good solution. The cost function result is shown in Fig. 7.
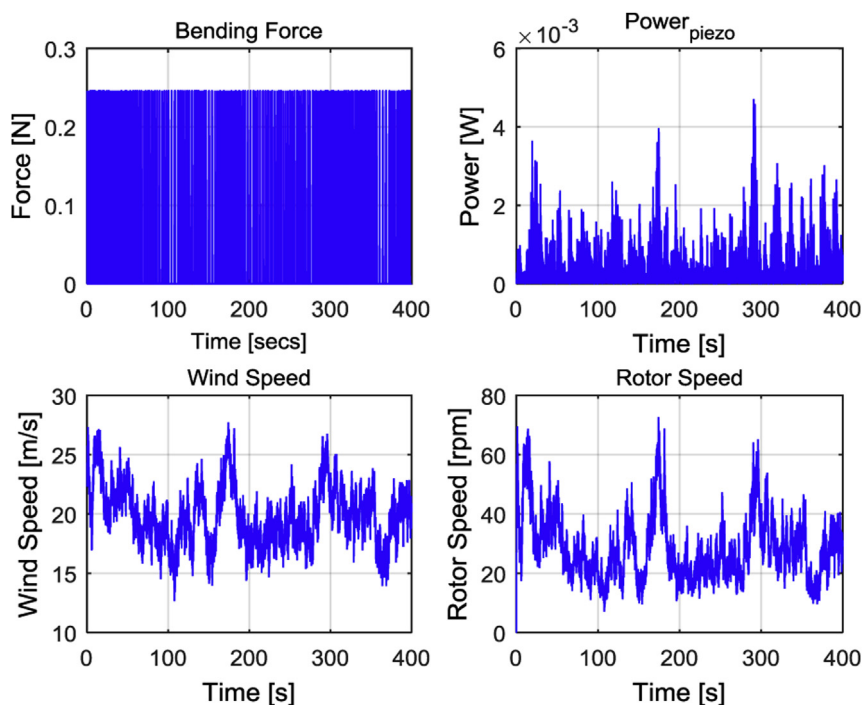
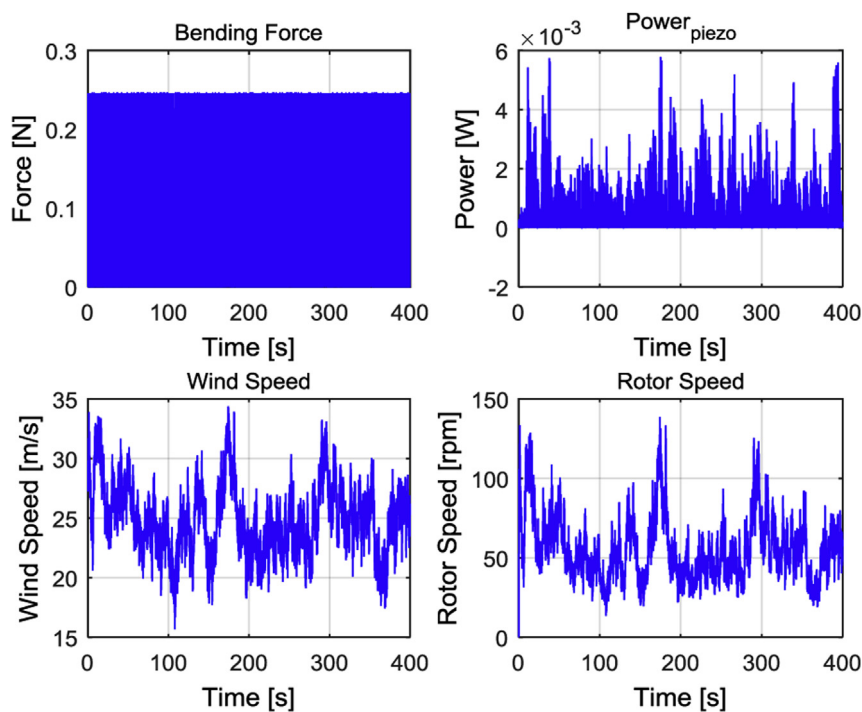Fig. 10 − Energy harvester response at 20 ms^{-1} wind speed.

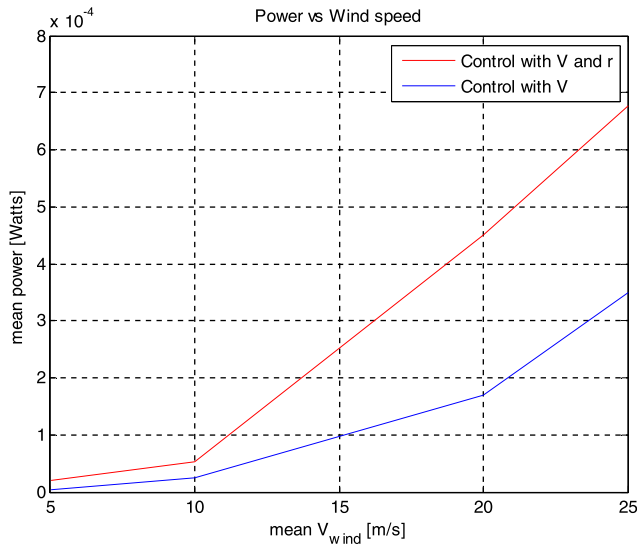Fig. 11 − Energy harvester response at 25 ms^{-1} wind speed.

Fig. 12 — Comparison between the mean power captured with the control proposed in Eq. (9) (red) and the control proposed in Ref. [21], that depends only on voltage (blue). (For interpretation of the references to color in this figure legend, the reader is referred to the web version of this article.)

Fig. 13 — Comparison between the mean bending force with the control proposed in Eq. (9) (red) and the control proposed in Ref. [21], that depends only on voltage (blue). (For interpretation of the references to color in this figure legend, the reader is referred to the web version of this article.)
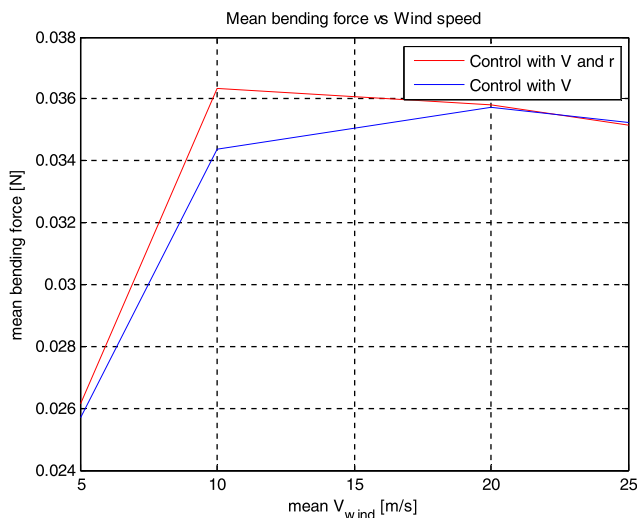
Results and discussion

After applying the optimization algorithm to the control system, we have obtained the following optimal values given by Eq. (19):

$$X_{global\ optimal} = \begin{cases} Kp_v = 5.9 \times 10^{-4} \\ Kp_r = -6.8 \times 10^{-5} \end{cases} \tag{19}$$

These two values of the parameters have been applied to the model with 400 s of time span in the simulations. Besides, we have made some simulations to show how the new control law introduces improvements compared with the control law proposed in Ref. [21]. We have made the comparisons with Normal Turbulence Model (NTM) having the mean wind speeds of 5 ms^{-1}, 10 ms^{-1}, 20 ms^{-1} and 25 ms^{-1}.

The system has a low power production at 5 ms^{-1} mean wind speed, but in comparison with the control law proposed in Ref. [21], the harvester mean power increases of 422%. On the other hand, the mean bending force increases with a low rate of 1.79%. The results are shown in Figs. 8, 12 and 13. In Fig. 8 we can verify that the harvester has good response in long time span (400 s).

The power production increases at 10 ms^{-1} mean wind speed and if we compare with the control law proposed in Ref. [21], the harvester mean power increases a 116.9%, while the mean bending force increases a rate of 5.71%, as show Figs. 9, 12 and 13. In Fig. 9 we can also verify that the harvester has good response in long time span (400 s).

The power increases up to very high levels at 20 ms^{-1} mean wind speed in comparison with the control law proposed in Ref. [21]. Besides, the harvester mean power increases a 164.15% at 20 ms^{-1} mean wind speed, while the mean bending force increases only a 0.118%, as detailed in Figs. 10, 12 and 13. In Fig. 10, we can assess that the harvester has good response in long time span (400 s) as in the previous cases.

A great power gain is achieved at the mean wind speed of 25 ms^{-1}. The harvester mean power increases a rate of 93.85% and the mean bending force decreases with a very low rate of 0.26%, as shown in Figs. 11—13. It is proven that the harvester has also a good response in long time span (400 s) through Fig. 11.

In Figs. 12 and 13 the results of the present exploration are summarized. The mean captured power has a really good increase in all wind speeds. Besides, the mean bending force has very low increase too up to a specific wind speed, being that result reasonable, since the piezoelectric layer has its own natural frequency and if the rotation rate of the harvester shaft (i.e., wind speed) differs too much from that natural frequency, the bending force cannot be so effective. Thus, as a general rule, the bending force will decrease by the magnetic force for some wind speed values. That also proves that the model is accurate enough and even for much higher wind speeds one can have lower power from the system as a result of that bending characteristics.

Conclusions

In this paper we have introduced a new control law with two inputs (i.e., voltage and bending deflection), and we have carried out a swarm optimization procedure for these parameters. This algorithm has been applied because there is no analytic relationship between the mean captured power and the control parameters. Furthermore, another important aspect in this study is to keep the bending force as low as possible in order not to break down the piezoelectric beam. It has been proven that these objectives have been achieved and the harvester power has been explored for a number of wind

mean speeds due to the new control law and optimization scheme. The wind speed has been performed by Turbsim tool and the current optimization and control strategies can be applied in other wind realizations or profiles. So, the main findings of the paper are the following: On one hand, a new control law based on both bending deflection and piezoelectric voltage has been designed; on the other hand, the tuning of the control parameters has been performed through a PSO optimizer.

Acknowledgments

REFERENCES

[1] Daoutidis P, Zachar M, Jogwar SS. Sustainability and process control: a survey and perspective. J Process Control 2016;44:184—206. http://dx.doi.org/10.1016/j.jprocont.2016.06.002.

[2] Parisio A, Rikos E, Glielmo L. Stochastic model predictive control for economic/environmental operation management of microgrids: an experimental case study. J Process Control 2016;43:24—37. http://dx.doi.org/10.1016/j.jprocont.2016.04.008.

[3] Wanga X, Teichgraeber H, Palazoglua A, El-Farraa Nael H. An economic receding horizon optimization approach for energy management in the chlor-alkali process with hybrid renewable energy generation. J Process Control 2014;24(8):1318—27. http://dx.doi.org/10.1016/j.jprocont.2014.04.017.

[4] Bouzelata Y, Altin N, Chennia R, Kurt E. Exploration of optimal design and performance of a hybrid wind-solar energy system. Int J Hydrogen Energy 2016;41(29):12497—511. http://dx.doi.org/10.1016/j.ijhydene.2015.12.165.

[5] Özcan EC, Erol S. A multi-objective mixed integer linear programming model for energy resource allocation problem: the case of Turkey. Gazi Univ J Sci 2014;27(4):1157—68.

[6] Bandyopadhyay S, Chandrakasan AP. Platform architecture for solar, thermal, and vibration energy combining with MPPT and single inductor. IEEE J Solid State Circuits 2012;47(9):2199—215. http://dx.doi.org/10.1109/JSSC.2012.2197239.

[7] Brunelli D, Moser C, Thiele L. Design of a solar-harvesting circuit for batteryless embedded systems. IEEE Trans Circuits Syst I: Regul Pap 2009;56(11):2519—28. http://dx.doi.org/10.1109/TCSI.2009.2015690.

[8] Dini M, Romani A, Filippi M, Bottarel V, Ricotti G, Tartagni M. A nanocurrent power management IC for multiple heterogeneous energy harvesting sources. IEEE Trans Power Electron 2015;30(10):5665—80. http://dx.doi.org/10.1109/TPEL.2014.2379622.

[9] Lopez-Lapena O, Penella MT, Gasulla M. A closed-loop maximum power point tracker for subwatt photovoltaic panels. IEEE Trans Ind Electron 2012;59(3):1588—96. http://dx.doi.org/10.1109/TIE.2011.2161254.

[10] Kamat PV. Quantum dot solar cells. Semiconductor nanocrystals as light harvesters. J Phys Chem C 2008;112(48):18737—53. http://dx.doi.org/10.1021/jp806791s.

[11] Wu Y, Zuo L, Zhou W, Liang C, McCabe M. Multi-source energy harvester for wildlife tracking. In: Active and passive smart structures and integrated systems 2014, vol. 9057; 2014. p. 905704. http://dx.doi.org/10.1117/12.2045139.

[12] Roundy S, Wright P, Rabaey J. Energy scavenging for wireless sensor networks with special focus on vibrations. 2004. p. 1—26.

[13] O'Donnell R. Energy harvesting from human and machine motion for wireless electronic devices. Proc IEEE 2008;96(9):1455—6. http://dx.doi.org/10.1109/JPROC.2008.927493.

[14] Kurt E, Uzun Y, Durmus C. Power characteristics of a new contactless piezoelectric harvester. 2015. http://dx.doi.org/10.1109/EPECS.2015.7368495.

[15] Uzun Y, Kurt E. The effect of periodic magnetic force on a piezoelectric energy harvester. Sensors Actuators A: Phys 2013;192:58—68. http://dx.doi.org/10.1016/j.sna.2012.12.017.

[16] Cottinet PJ, Guyomar D, Guiffard B, Putson C, Lebrun L. Modeling and experimentation on an electrostrictive polymer composite for energy harvesting. IEEE Trans Ultrason Ferroelectr Freq Control 2010;57(4):774—84. http://dx.doi.org/10.1109/TUFFC.2010.1481.

[17] Patel I, Siores E, Shah T. Utilisation of smart polymers and ceramic based piezoelectric materials for scavenging wasted energy. Sensors Actuators A: Phys 2010;159(2):213—8. http://dx.doi.org/10.1016/j.sna.2010.03.022.

[18] Vatansever D, Hadimani RL, Shah T, Siores E. An investigation of energy harvesting from renewable sources with PVDF and PZT. Smart Mater Struct 2011;20(5):055019. http://dx.doi.org/10.1088/0964-1726/20/5/055019.

[19] Ronkanen P, Kallio P, Vilkko M, Koivo HN. Displacement control of piezoelectric actuators using current and voltage. IEEE-ASME Trans Mechatron 2011;16(1):160—6. http://dx.doi.org/10.1109/TMECH.2009.2037914.

[20] Uzun Y, Demirbas S, Kurt E. Implementation of a new contactless piezoelectric wind energy harvester to a wireless weather station. Elektron Ir Elektrotechnika 2014;20(10):35—9. http://dx.doi.org/10.5755/j01.eee.20.10.8871.

[21] Zulueta E, Kurt E, Uzun Y. Control law determination for a new contactless piezoelectric wind energy harvester. In: IV European conference on renewable energy systems, ECRES2016, Istanbul, Turkey; 2016. p. 841—7.

[22] NWTC Information Portal (TurbSim). https://nwtc.nrel.gov/TurbSim. Last modified 14-June-2016; [Accessed 22 January 2017].

[23] Iliuk I, Balthazar JM, Tusset AM, Piqueira JRC, de Pontes BR, Felix JLP, et al. Application of passive control to energy harvester efficiency using a nonideal portal frame structural support system. J Intell Mater Syst Struct 2014;25(4):417—29. http://dx.doi.org/10.1177/1045389X13500570.

[24] Brasil RMLRF, Feitosa LCS, Balthazar JM. A nonlinear and non-ideal wind generator supporting structure. In: Modern practice in stress and vibration analysis VI, proceedings, vols. 5—6; 2006. p. 433—42.

[25] Abdelkefi A, Hajj MR, Nayfeh AH. Sensitivity analysis of piezoaeroelastic energy harvesters. J Intell Mater Syst Struct 2012;23(13):1523—31. http://dx.doi.org/10.1177/1045389X12440752.

[26] Balthazar JM, Tusset AM, Bueno AM. Tm-afm nonlinear motion control with robustness analysis to parametric errors in the control signal determination. J Theor Appl Mech 2014;52(1):93—106.

[27] Shen W, Zhu S. Harvesting energy via electromagnetic damper: application to bridge stay cables. J Intell Mater Syst Struct 2015;26(1):3—19. http://dx.doi.org/10.1177/1045389X13519003.

[28] Pereira MFV, Balthazar JM, Dos Santos DA, Prado I. A note on polynomial chaos expansions for designing a linear feedback control for nonlinear systems. Nonlinear Dyn 2017;87(3):1653—66. http://dx.doi.org/10.1007/s11071-016-3140-3. Available:.

[29] Balthazar JM, Bassinello DG, Tusset AM, Madureira Bueno A, Rodrigues de Pontes Jr B. Nonlinear control in an electromechanical transducer with chaotic behaviour. Meccanica 2014;49(8):1859—67. http://dx.doi.org/10.1007/s11012-014-9910-4.

[30] Tummala A, Kishore Velamati R, Kumar Sinha D, Indraja V, Hari Krishna V. A review on small scale wind turbines. Renew Sustain Energy Rev 2016;56:1351—71. http://dx.doi.org/10.1016/j.rser.2015.12.027.

[31] Gonzalez-Gonzalez A, Etxeberria-Agiriano I, Zulueta E, Oterino-Echavarri F, Lopez-Guede JM. Pitch based wind turbine intelligent speed setpoint adjustment algorithms. Energies 2014;7(6):3793—809. http://dx.doi.org/10.3390/en7063793.

[32] Jiang Lu X, Li Han-Xiong, Yuan X. PSO-based intelligent integration of design and control for one kind of curing process. J Process Control 2010;20(10):1116—25. http://dx.doi.org/10.1016/j.jprocont.2010.06.019.

[33] Gharavian D, Pardis R, Sheikhan M. ZEBRA battery SOC estimation using PSO-optimized hybrid neural model considering aging effect. IEICE Electron Express 2012;9(13):1115—21. http://dx.doi.org/10.1587/elex.9.1115.

[34] Qin Y, Peng H, Ruan W, Wu J, Gao J. A modeling and control approach to magnetic levitation system based on state-dependent ARX model. J Process Control 2014;24(1):93—112. http://dx.doi.org/10.1016/j.jprocont.2013.10.016.

[35] Oterino-Echavarri F, Zulueta E, Ramos-Hernanz J, Calvo I, Lopez-Guede JM. Application of differential evolution as method of pitch control setting in a wind turbine. In: International conference on renewable energies and power quality (ICREPQ'13), Bilbao (Spain); 2013. ISSN 2172—038 X, No.11.,.

[36] Civicioglu P. Backtracking search optimization algorithm for numerical optimization problems. Appl Math Comput 2013;219(15):8121—44. http://dx.doi.org/10.1016/j.amc.2013.02.017.

[37] Trong Tai N, Ahn KK. A hysteresis functional link artificial neural network for identification and model predictive control of SMA actuator. J Process Control 2012;22(4):766—77. http://dx.doi.org/10.1016/j.jprocont.2012.02.007.

[38] Kennedy J, Eberhart R. Particle swarm optimization. 1995. http://dx.doi.org/10.1109/ICNN.1995.488968.

[39] Jabria K, Dumur D, Godoy E, Mouchette A, Bèle B. Particle swarm optimization based tuning of a modified smith predictor for mould level control in continuous casting. J Process Control 2011;21(2):263—70. http://dx.doi.org/10.1016/j.jprocont.2010.10.019.

[40] Bechouat M, Soufi Y, Sedraoui M, Kahla S. Energy storage based on maximum power point tracking in photovoltaic systems: a comparison between GAs and PSO approaches. Int J Hydrogen Energy 2015;40(39):13737—48. http://dx.doi.org/10.1016/j.ijhydene.2015.05.008.

[41] Behera S, Subudhi B, Pati B. Design of PI controller in pitch control of wind turbine: a comparison of PSO and PS algorithm. Int J Renew Energy Res 2016;6(1):271—81.

[42] Salih HW, Wang S, Farhan BS. PSO tuned fuzzy based pitch blade controller of grid-tied variable speed wind turbine. 2016. http://dx.doi.org/10.1109/ICIEA.2016.7603679.

[43] Shunzhi M, Shunyuan S, Baoguo X. Wireless sensor networks non-uniform clustering and dcluster heads routing algorithm based on PSO. Chin J Sensors Actuators 2014;27(9):1281—6. http://dx.doi.org/10.3969/j.issn.1004-1699.2014.09.022.

[44] Zeddini MA, Pusca R, Sakly A, Mimouni MF. PSO-based MPPT control of wind-driven self-excited induction generator for pumping system. Renew Energy 2016;95:162—77. http://dx.doi.org/10.1016/j.renene.2016.04.008.